

# Modified Perturb and Observe MPPT Algorithm for Partial Shading Conditions

Muhammad Rayyan Fazal<sup>\*‡</sup>, Zaheer Abbas<sup>\*\*</sup>, Muhammad Kamran<sup>\*</sup>, Inzamam ul Haq<sup>\*</sup>, Muhammad Naeem Ayyaz<sup>\*\*\*</sup>, Muhammad Mudassar<sup>\*\*\*\*</sup>

\* Department of Electrical Engineering and Technology, Riphah International University, Faisalabad, Pakistan.

\*\* Department of Electrical Engineering, University of Engineering and Technology, Lahore, Pakistan.

\*\*\* Department of Computer Science, NAMAL Institute, Mianwali, Pakistan.

\*\*\*\* Department of Technology, The University of Lahore, Lahore, Pakistan

(rayyan.m@yahoo.com, zee.elect@gmail.com, kamran\_ramzan@outlook.com)

‡Corresponding Author; Muhammad Rayyan Fazal, Tel: +92 300 786 9321, rayyan.m@yahoo.com

*Received: 08.02.2019 Accepted: 10.03.2019*

**Abstract-** Tracking the maximum power output is significantly important for the optimized photovoltaic operation. Maximum power point (MPP) is never constant and directly depends upon the solar irradiance and temperature of the cell. Hence, it is primordial to employ any technique to track MPP. This paper uses a modified Perturb and Observe (P&O) algorithm based on the Global Maximum Power point (GMPP) for a standalone photovoltaic system. It turns out to be a novel, simpler and efficient approach to accommodate the aforementioned problem and efficiently track MPP under varying climatic conditions. Simulation results verify the effectiveness of our proposed scheme in terms of accuracy, tracking time, robustness, simplicity and efficiency under static and dynamic atmospheric circumstances. Under normal conditions, MPP is tracked within 0.1 seconds, while for partial shading, GMPP is tracked within 0.15 seconds with an efficiency of 99.19%.

**Keywords:** Maximum Power Point Tracker (MPPT), Photovoltaic (PV) Systems, Perturb and Observe (P&O), Solar.

## 1. Introduction

The earth receives a force of around  $1.8 \times 10^{11}$  MW, directly from the sun [1]. Sun is the most sustainable, plentiful, maintenance-free and pollution-free source of energy and it is now the hottest research topic. However, solar energy has several drawbacks that limit its widespread use. In this regard, relatively high production and installation costs, storage depreciation, and especially low conversion efficiency are some of the key hurdles to overcome the widespread use of solar energy. In addition, because solar energy from the sun is not always constant throughout the day, we must devise efficient and practical techniques to capture the greatest, matchless and abundant energy of all the times [2].

Over the past years, several MPPT technologies have been established and used that have different costs, convergence, tracking speed, software/hardware application and different methodologies. Some of the most reliable methods so far for researchers and PV industrial corporations are climbing, Perturbation, and Observation (P&O), conductance method and fractional-open-circuit voltage method [3].

The P&O technique involves perturbations in the operational PV array voltage, while the climbing method

includes perturbations in the duty cycle of any power converter. Both techniques are distinct means of envisioning the same basic methodology because the output from PV array is unswervingly troubled through the duty cycle and/or effective voltage [4]. For example, Figure 1 elaborates the phenomena through I-V and P-V curves taken from a solar cell module. It has been provided with the open circuit (OC) voltage at 1000 W/m solar radiations with  $V_{OC} = 21.6V$  with short-circuit (SC) current of  $I_{SC} = 5A$ . The voltage increases in small-scale steps, the calculated power is stored, whereas, the next perturbation takes the direction that depends upon the difference between values of current and the preceding power value to trace MPP.

The incremental conductance technique takes the sign ( $dP/dV$ ) of the P-V curve slope, i.e., 0 at MPP. As it is positive at the left side of the MPP, and negative at the right. Whereas, in fractional-open-circuit voltage technique, the effective voltage is considered to be an immovable portion of  $V_{OC}$  of the array, irrespective of the input/output settings. Though, considering some shielding of the PV system, P-V and/or I-V curves do not have a single MPP. Moderately, multiple peaks depend on the pattern of shading (s). In our scenario of multiple MPPs, various tracking methods described above do not converge towards GMPP and also offers complex modeling. So, we have to adopt better technology to solve this problem.

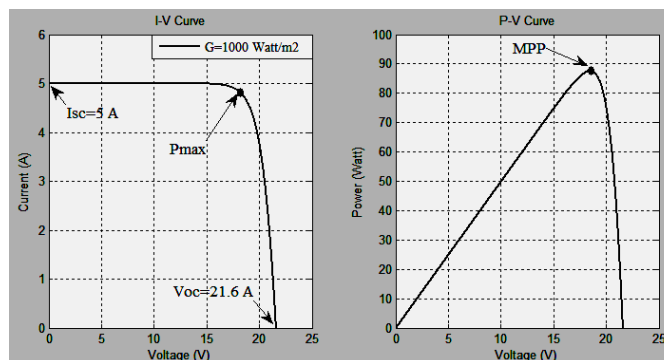


Fig. 1: I-V/P-V curves of a PV module

GMPP tracking of partly shaded PV structures has widely studied in the literature. Various techniques are compared in terms of their partial shading response and effectiveness of PV modules and energy outputs [5-7]. Researchers reviewed a variety of MPPT technologies such as power-curve slope methods for finding GMPP, instantaneous operating power optimization, load-line tracking, power boosting techniques, neural networks, Fibonacci search, and particle group optimization (PGO). In the power-curve slope method, since the GMPP is blindly alarmed on any side of local MPP [8], the partial shading condition suddenly changes with the tracking speed not fast enough. Load track tracking only applies to certain shaded patterns and has a high error rate. The percentage error for the power increase technique that uses particle swarm optimization (PSO) is relatively small, but at the same time, the tracking frequency is small too [9]. An improvement in the performance of a PV solar panel is observed under dynamic climatic conditions when adaptive Neuro-fuzzy interference system is applied that is based on the MPPT [10]. Immediate operating power optimization is quite fast to track GMPP, but the difficulty associated is the pre-evaluation of current at further extreme values. The Fibonacci search seems likely to the P&O technique, excluding for the modification in step size selected by the Fibonacci arrangement, so this method can deceive local maxima relatively to global ones. Neural network technology illustrates the satisfactory speed and accurateness, but it is contingent on the arrangement and needs an isolated sensor for energy measurement [11-13]. Hardware implementation based study, that uses incremental conductance MPPT is observed to provide 33% PV output efficiency [10]. Particle cluster optimization has alike construction to the hill-climbing method, but this procedure shows a composite execution and needs a commanding microcontroller for digital application [14].

A novel method showed the effectiveness of the two-staged PSO algorithm, under shading conditions, for cascaded PV-modules. However, the complexity and extra time involved restrict its further implementation [15]. A novel technique for improved transient response through derivative control is suggested. It is proved that, as bus voltage fluctuates, the range of PV panel is improved by 80% [16]. Whereas this technique is further modified and improved for a quicker response to the abrupt atmospheric changes [17]. P&O algorithm for MPPT with confined space

search approach is also found to be an effective approach [18]. A. Zbeeb et al. Tracked GMPP using primary and secondary derivatives as a meaning of the duty cycle. This algorithm emphasis on unexpected changes in the air and does not deliver a way to path GMPP [19].

Investigators have used essentially two methods of finding global MPPs. Both methods used the entire P-V or I-V curve as a global/blind scanning approach. It makes it overall a complex and time-consuming way that uses heavy calculations and affluent hardware based specialized devices. Whereas our current work established a new, simpler, and efficient method to track MPP by solving and overcoming the aforementioned problems. Moreover, this algorithm is found to be more accurate and efficient that can track the global maximum power point (GMPP) in dynamic input/output conditions.

## 2. The Behavior of MPP under Variant Conditions

MPP is greatly affected due to several factors including variable irradiancies, output loading, and partial shading. The following section discusses and simulates the effects of all these parameters in MATLAB / Simulink.

### 2.1. Influence of solar radiation/corrosion resistance on MPP

The power is directly proportional to the survey level ( $W/m^2$ ). The resultant radiations are quite noticeable at short-circuiting currents, however, not at the open-circuit voltage of the PV system. For example, Figure 2 demonstrates the pretentiousness of MPP, if irradiance changes from 200 to 1000  $W/m^2$ .

The increase in Solar irradiance increases the short circuit current of the solar PV cell. Hence, the PV cell temperature increases, as a result, its performance decreases. The increased temperature also decreases the open circuit voltage of the PV cell. In short, the maximum power point of the PV cell is reduced.

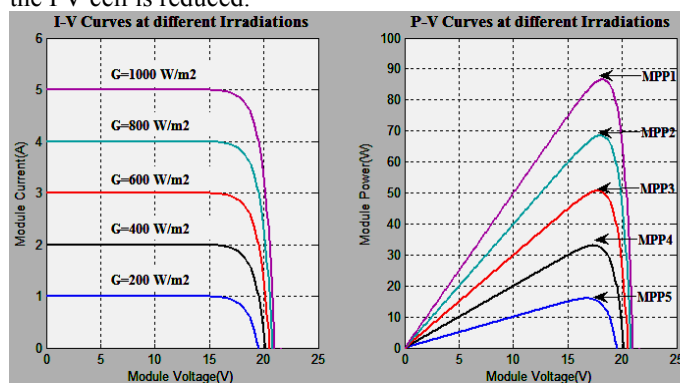


Fig. 2: I-V/P-V curves of a PV module at various solar irradiancies

### 2.2. The consequence of load resistance in MPP

The load linked to the output of the PV plant is not always constant. It changes rather on the claim. As a consequence, the operational fact of the PV structure

depends on the cost of the output load. For example, Figure 3 shows that increasing load resistance origins the PV output to rise for the first time, approaching the MPP value, and the output load resistance equals the exceptional value of the optimal resistance ( $R_{opt}$ ). Also, Load resistance increases with  $R_{opt}$  that decreases PV output intensely. Therefore, to obtain maximum output in a PV plant, the output resistance must be equal to the optimal value.

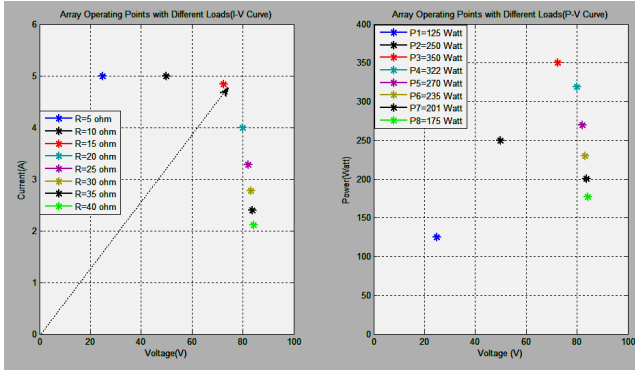


Fig. 3: operating points of I-V/P-V curves for distinct values of load resistance ( $R_L$ )

2.3. Partial shading effect in MPP

Four series arrays of modules are used in simulation purpose as exposed in Figure 4. The power productivity of PV scheme is conspicuously reduced when shading is performed on the smooth percentage of the PV collection. It is not necessary for the shadow to cover the entire module, whereas shading of even a single cell has the ability to bring down the output sharply, that in return affects the overall output of the string. Also, if there is an unshaded string, it continues to supply the power normally. For instance, if module cell 4 is shaded ( $500W/m^2$ ), but the remaining modules are subjected to uniform illumination ( $1000W/m^2$ ), the characteristic curve is plotted in Figure 5.

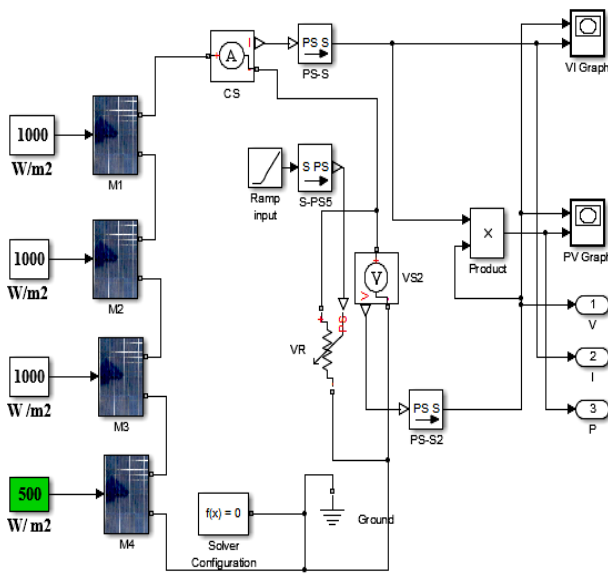


Fig. 4: Modelling of PV array

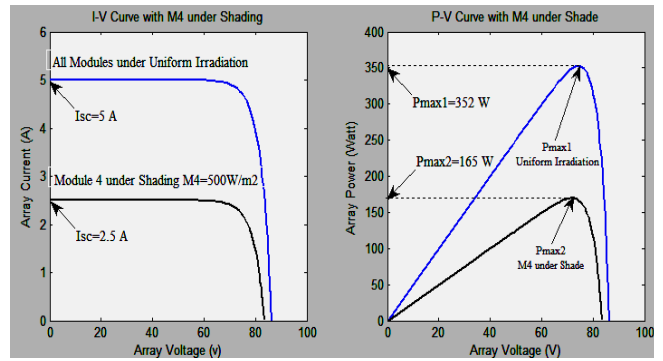
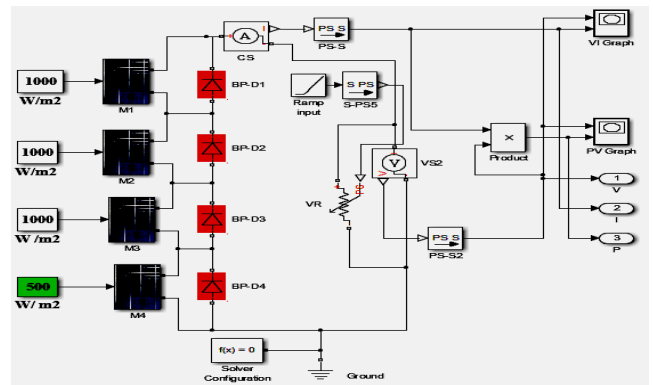
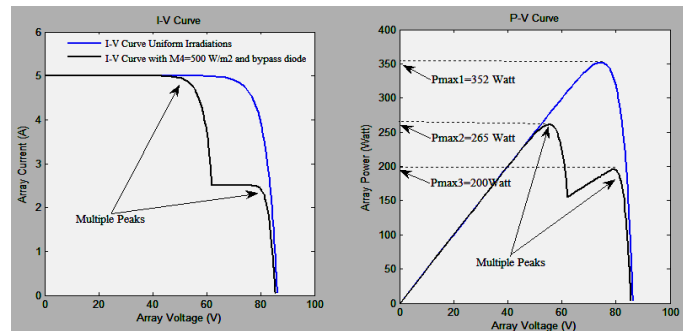


Fig. 5: I-V and P-V curves of a shaded (M4) PV array without a bypass diode



6(a)



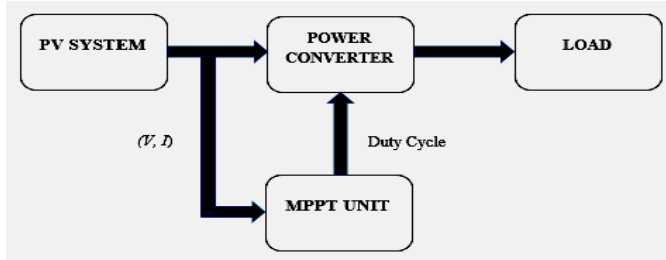
6(b)

Fig. 6: (a) Simulink model for partial shading with bypass diodes. (b) I-V/P-V curves of shaded (M4) and unshaded PV array using bypass diodes.

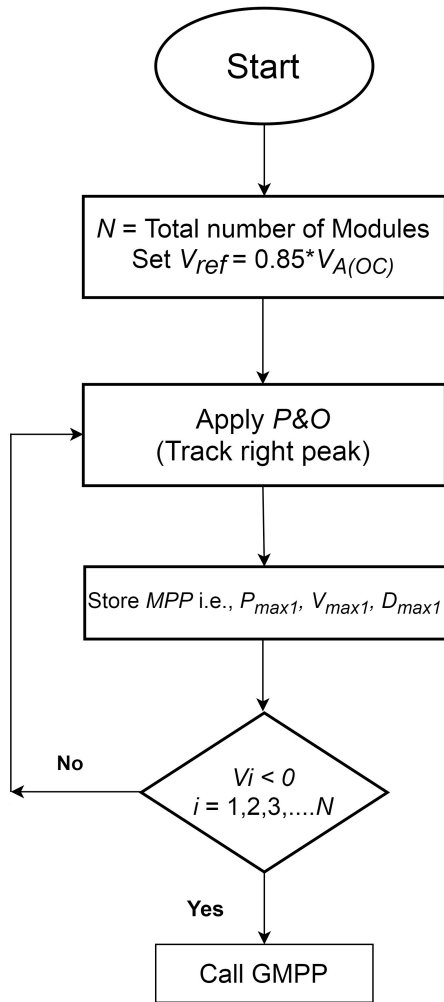
3. MPPT Algorithm and Equivalent Model

The basic purpose of MPPT is forcing the resistance of the PV array near to optimal values under all climatic conditions and varying output loads. By using the inherent characteristics of a DC/DC power converter, the input resistance is made dependent upon the duty cycle ( $D$ ) because the output resistance of the array cannot be continuously adjusted as the weather conditions change. Regardless of the load resistance, MPPT (duty cycle adjustment) retains the resistance seen at PV array at the optimal value. A flow chart of a comprehensive PV system through our suggested algorithm is given away in Figure 7.

The photovoltaic system consists of a solar PV module, a DC-DC Power Electronic converter, and its control signal, that is decided by the maximum power point tracking Algorithm as shown in fig. 7 (a). the power converter could be a buck converter, boost convert, buck/boost, a flyback converter, forward converter or SEPIC converter. In the proposed MPPT model we have used a buck converter.



7(a)

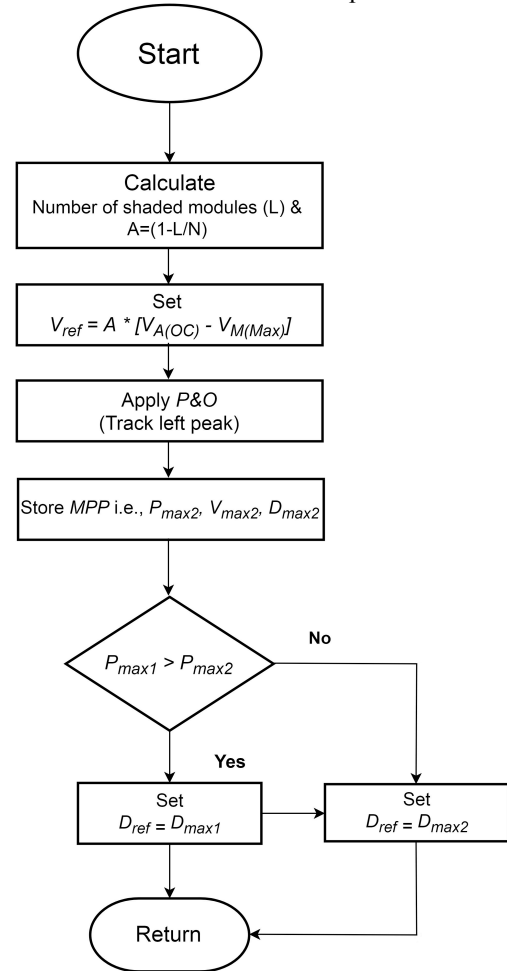


7(b)

N is the overall number of modules in Figure 7 (b), and  $V_{ref}$  is the reference voltage at which the agitation begins,  $V_A(OC)$  points to the open-circuit voltage of array, whereas  $V_i$  is the operating voltage corresponding to the  $i$ th module, the amount of  $V_{MS}$  (maximum) is the module voltage, supplying the maximum power. The projected algorithm consists of mainly two further parts: unchanging weather

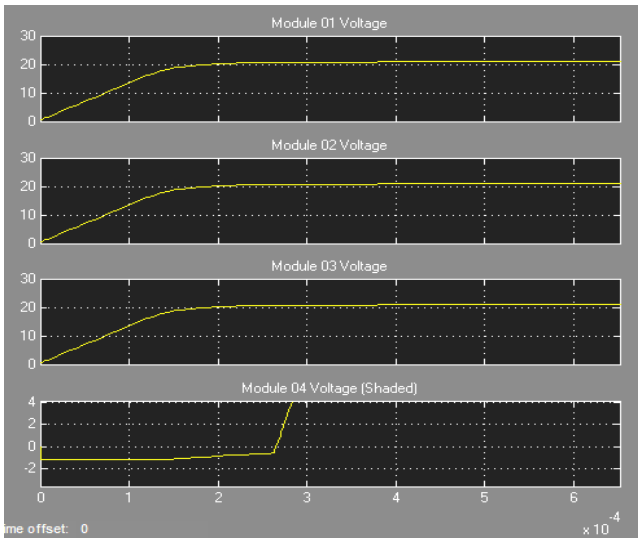
condition, the foremost algorithm (MPP) and partial shading, i.e., GMPP algorithm.

Note the algorithm starts by manipulating the total number of modules (N) and sets the orientation voltage ( $V_{ref}$ ) accordingly to 85% of collection voltage. The MPP is intended by applying the P&O and its price is kept (i.e.,  $P_{max1}$ ,  $V_{max1}$ ,  $D_{max1}$ ). The attendance of partial shading is sensed through perceiving the working voltage of a given module, as shown in Figure 8 (a). Figure 8 (c) shows that when M4 is under the shadow, the M4 voltage is equivalent to the negative value of the diode's forward voltage because M4 is not conducting and the bypass diode across M4 conducts. M4 also starts after point C, which can be seen in figure 8 (b). This is an identification of the shaded module's voltage that represents a partial shade that equals the negative of the diode's forward voltage until the end of the first peak. Partially shaded modules have voltages less than zero or lower voltages than normal modules, as shown in figure 9. The yellow line is for shading module and the magenta line is for the normal module. After detecting partial shading, and the GMPP is utilized to set a new  $V_{ref}$ , depending on the partially shaded area of modules (L). MPP (left peak) is pursued and values,  $P_{max2}$ ,  $V_{max2}$ ,  $D_{max2}$ , are stored. Finally,  $P_{max1}$  (right peak) and  $P_{max2}$  (left peak) are compared and the resultant value is the peak.



7(c)

Fig. 7: (a) Block diagram of the complete PV system, (b) and (c) flow chart of our proposed algorithm



(a)

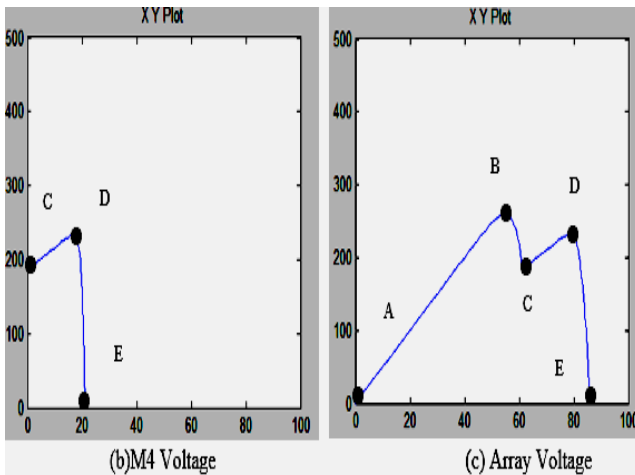


**Fig. 8:** (a) Module Voltages with M4 under Shade (b) M4 Voltage  $V_s$  Output power (c) Array Voltage  $V_s$  Output Power

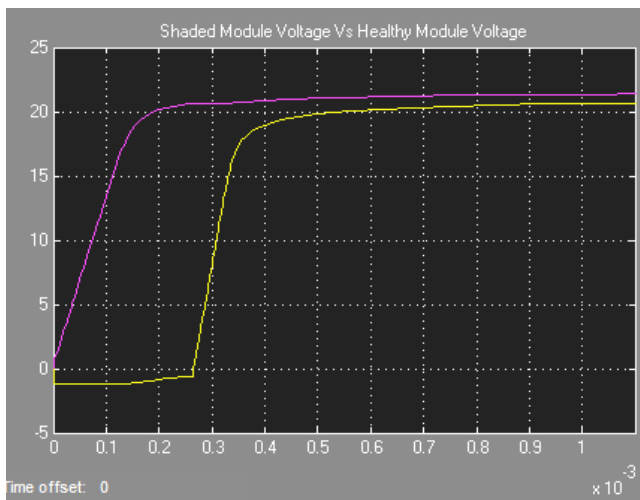


**Fig. 9:** Comparison of Module Voltages under Shading

Complete model based on the proposed algorithm is designed in Simulink. Current and voltage signals are being fed to the controller and in returns, it provides us with a

monitored duty cycle signal which is used to drive the average voltage-based DC/DC bridge buck converter. Duty cycle signal before entering the converter is limited between the values of 0 and 1 and then the scaling of the duty ratio signal is carried out. All the module voltages are also fed to the controller to identify the presence of the partial shading. Fig. 10 shows an MPPT controller that contains multiple blocks, switches, input and output ports. The controller receives the current and voltage signal and starts tracking the right peak by block no. 4. After a time, lapse, the presence of partial shading is sensed by block no.2 and the control is handed over to block no. 3 and the MPP of the left peak are tracked. Then both the MMP's are compared by block no. 5 and the control is transferred to whether block no.3 or 4 depending upon the powers of the two peaks. MPPT controller continuously tracks the MPP, hence, whenever the weather changes and shading occur, the controller senses it through the whole cycle described above and then responds accordingly. It adjusts the duty cycle in a quick manner to track the maximum power point efficiently.

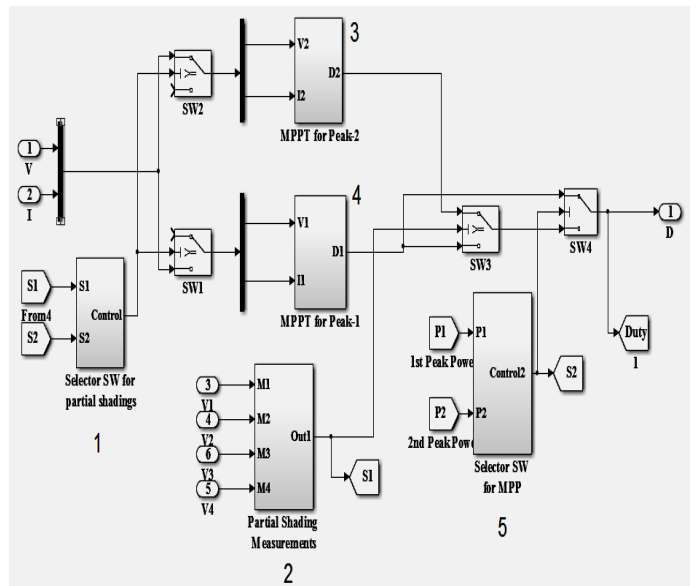


**Fig.10:** MPPT Controller

#### 4. Simulated Results

A comprehensive PV scheme is self-possessed of 4 modules linked in series. Fig. 11 shows the Simulink model having parameters:  $P_{max}=352$  W,  $V_{OC}=86.4$  V, and  $I_{SC}=5$  A and by means of the projected algorithm, an MPPT component is intended to combine with the DC/DC buck converter.

##### 4.1 Uniform Irradiation MPP

All modules should be beneath unchanging irradiation, i.e.,  $G = 1000$  W/m<sup>2</sup> with a load of  $1.63 \Omega$  ( $R_{opt}$ ) is linked. The orientation voltage is selected as  $V_{ref} = 0.85 * 86.4 = 73.44$ V. The simulation results are shown for 0.5 seconds in Fig. 12, with  $D = 0.34$ , and  $V_{PV} = 70.56$ V, the MPP is outlined in 0.1 second,  $I_{PV} = 4.98$  A, and  $P_{PV} = 352$  W.

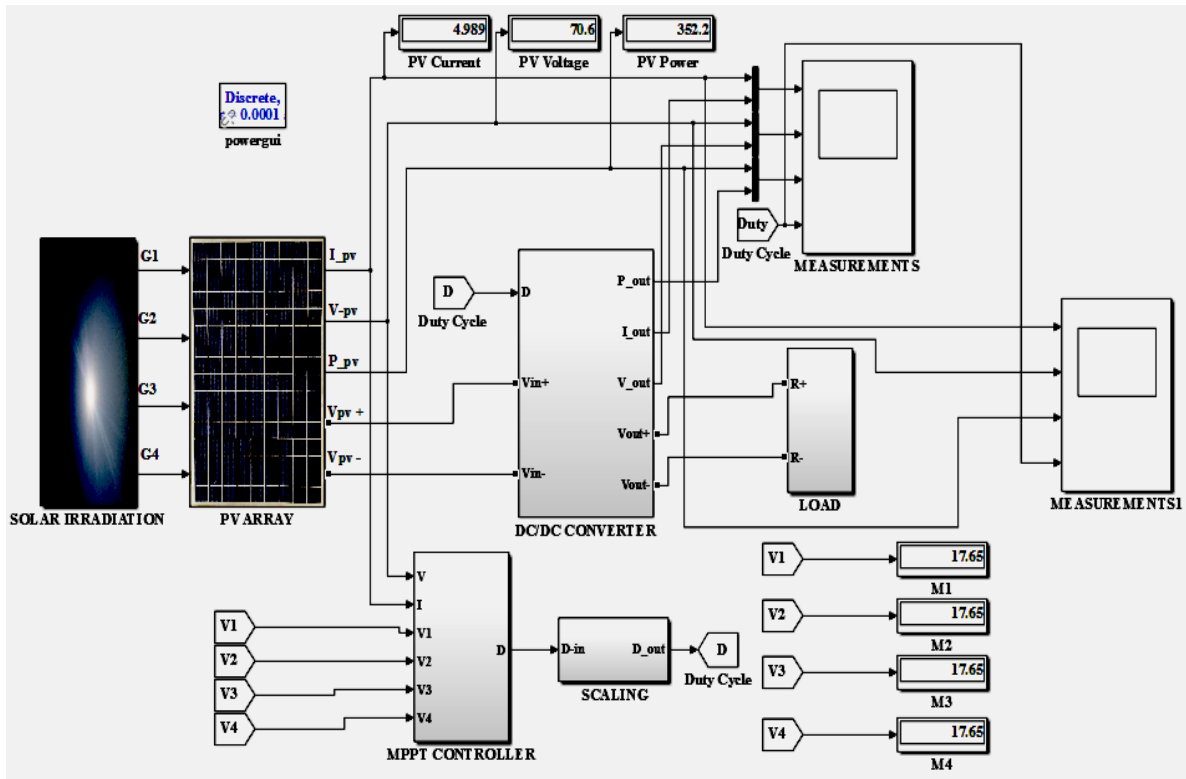


Fig. 11: Complete PV system with MPPT

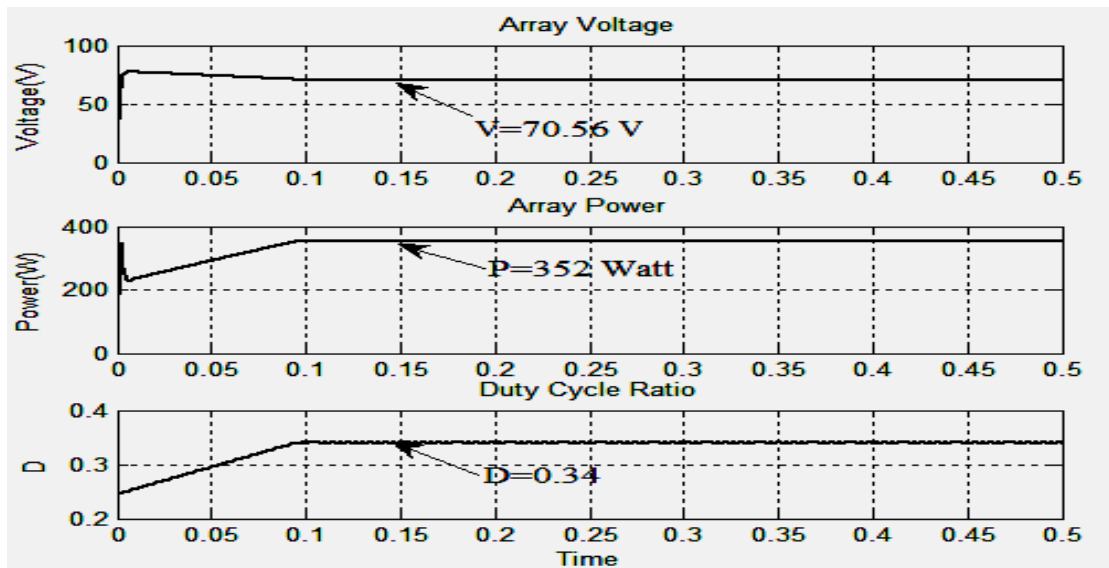


Fig. 12: PV array voltage, power and duty ratio under uniform irradiation ( $1000W/m^2$ )

4.2 MPP for sudden weather changes

It can be seen from fig. 13 that the irradiation is maintained at  $600 W/m^2$  with a duty cycle of 0.25 and a power of 230 W between 0 and 0.4 seconds. In 0.4 seconds, the weather suddenly changes, and the irradiation increases to  $800W/m^2$ . MPPT detected this variation and, subsequently a very petite period of time, attained a power output of 290 watts with a duty cycle relation of 0.29. After 0.7 seconds, the irradiation increases to  $1000 W/m^2$  and the power ranges the maximum value, 352 watts with the duty ratio of 0.34.

4.3 Under Load Variations, MPP

Connect the following three load resistors ( $R_1 = 1 \Omega$ ,  $R_2 = 3 \Omega$ ,  $R_3 = 5 \Omega$ ) with solar irradiation fixed at  $1000W/m^2$ .

- 1) 0 ~ 0.3 sec.  $R_L = R_1$
- 2) After 0.3 seconds.  $R_L = R_1 \parallel R_2$
- 3) After 0.6 seconds  $R_L = R_1 \parallel R_2 \parallel R_3$

In the simulation results (Figure 14), it can be seen that MPPT kept the power extracted from the PV array under all load resistor combinations at an optimum value of 352 watts by adjusting the duty cycle ratio appropriately.

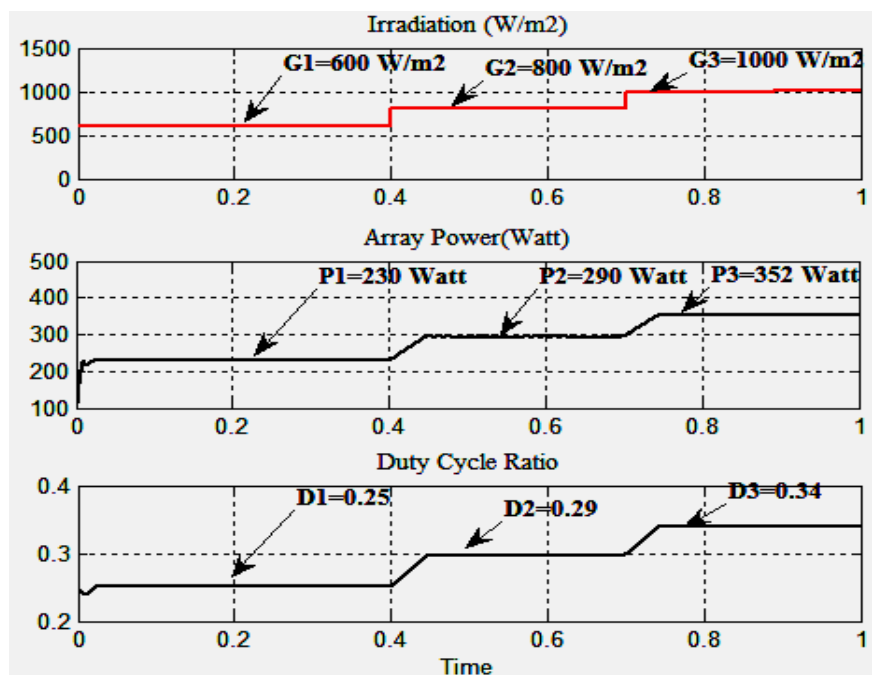


Fig. 13: PV array power and duty ratio under abrupt changing weather

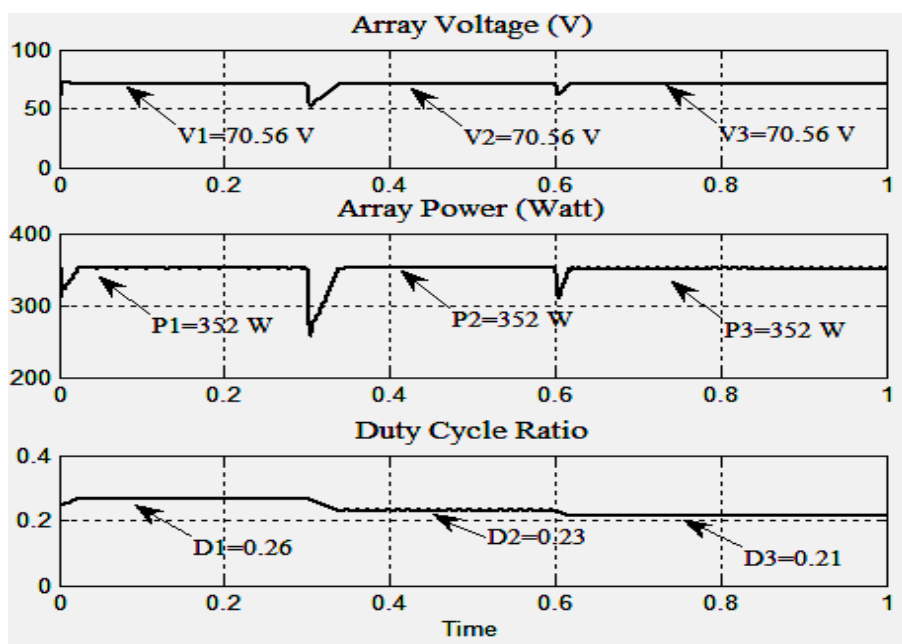


Fig. 14: PV array voltage, power and duty ratio under changing loads

#### 4.4 MPP under Partial Shading

In this unit, approximately the modules were shaded (low dose) and GMPP was traced if there were multiple maximum values.

##### Case-1: M4 is shielded (600 W/m<sup>2</sup>)

Rendering to the MPP algorithm, the voltage for the correct peak is set at 73.44V and the MPP at the right peak ( $P_{max1} = 230\text{Watt}$ ) is tracked (see Figure 15). As soon as partial shading is noticed, the switch is passed to the GMMP algorithm, the left peak orientation voltage is set to  $(1 - 1/4)$

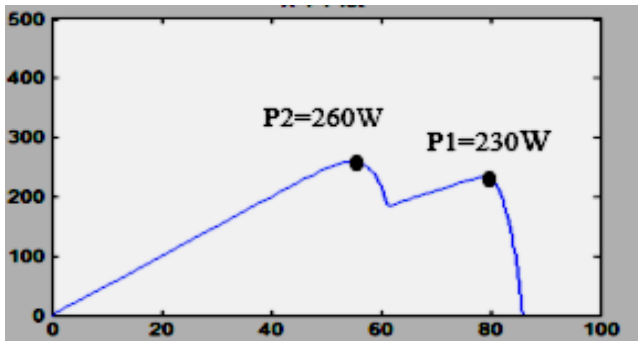
\*  $(86.4 - 17.56) = 51.63\text{V}$ , and the left peak ( $P_{max2} = 260\text{W}$ ) is tracked. The comparison is then complete and the duty cycle and voltage for the higher peak ( $P_{max2} = 260\text{ Watt}$ ) is set as a reference.

##### Case-2: M4 and M3 are under shade (600 W/m<sup>2</sup>)

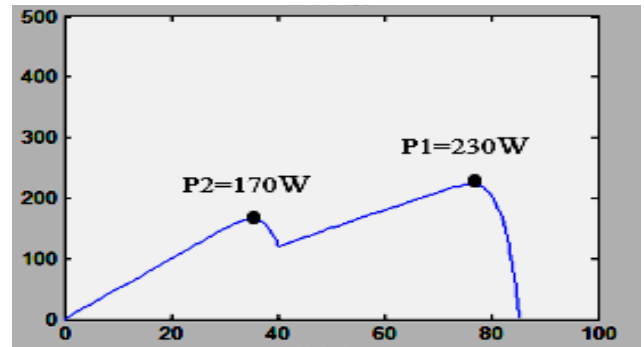
M3 and M4 are kept under shade (600 W/m<sup>2</sup>) and the simulation results are shown in Figure 16. Using M4 and M3 shades, two peaks are formed, the power of the right peak is  $P_{max1} = 230\text{W}$  and the peak of the left peak is  $P_{max2} = 170\text{ watts}$ . From the simulation results, you can see that MPPT tracks the correct peak and then traces to the left. After

comparison, the voltage and duty cycle of the higher peak ( $P_{max1} = 230$  Watt) is set as a reference.

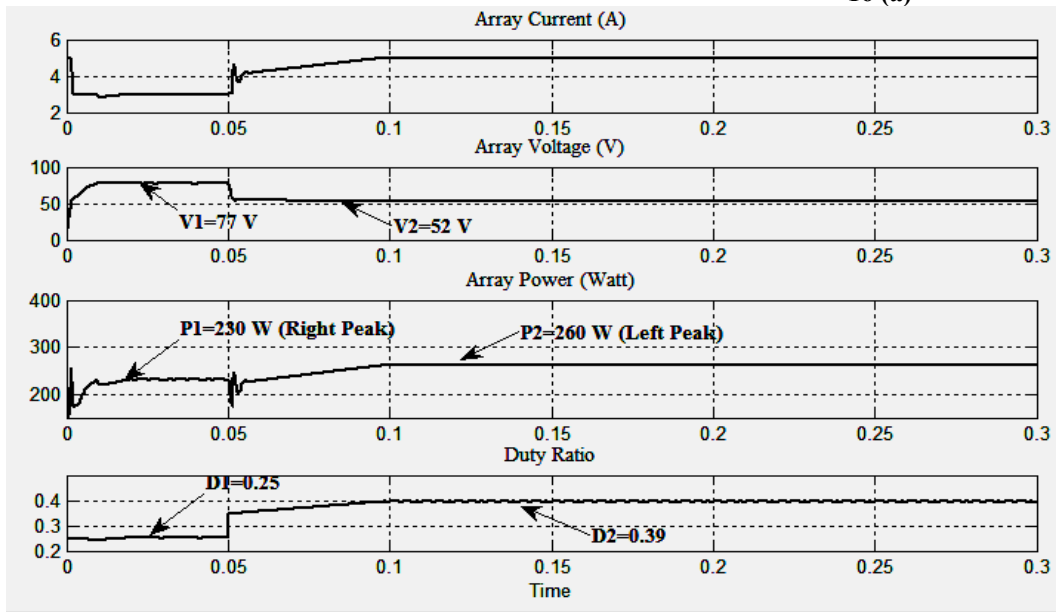
To sum up, a detailed comparison of various MPPT techniques, including our proposed one, has been provided in Table 1.



15(a)

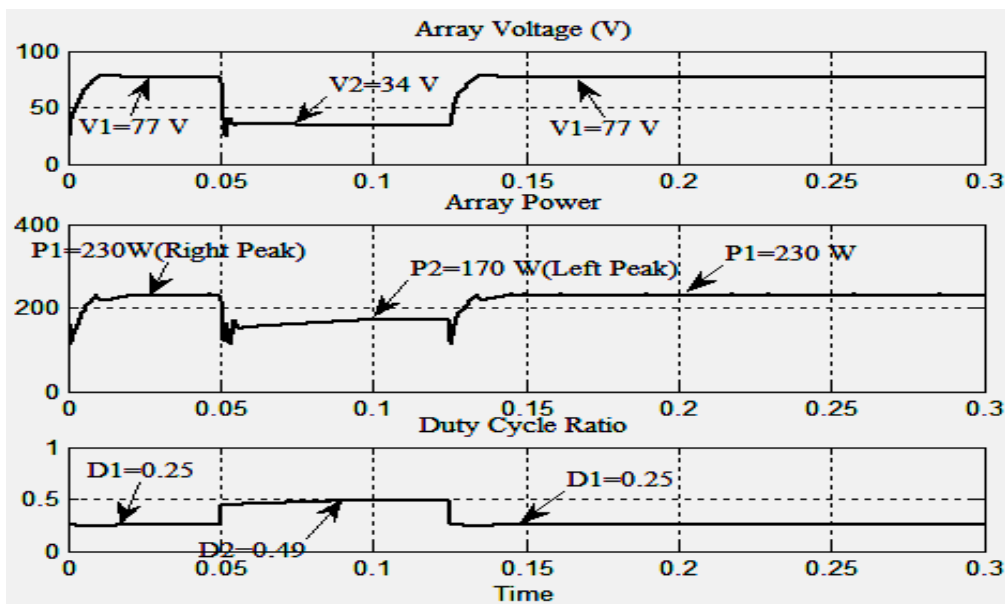


16 (a)



15(b)

Fig.15: (a) P-V curve with M4 under shade (b) PV array voltage, power and duty ratio with M4 under shade ( $600W/m^2$ )



16 (b)

Fig. 16: (a) P-V curve with M3&M4 under shade (b) PV array voltage, power and duty ratio with M4 and M3 under shade ( $600W/m^2$ )



**Table 1:** Comparison of various MPPT techniques.

Ref.	MPPT technique	Control variable	Converter type	Observations
Proposed	GMPP based P&O	Duty cycle	DC/DC Buck converter	This algorithm is faster, simpler and more precise than the existing algorithms. GMPP is tracked more efficiently in static and dynamic atmospheric conditions.
(Kamran et al. 2018) [18]	Confined search spaced P&O	Duty cycle	Boost converter	This paper proposes a modified P&O algorithm integrated with dual axis solar tracker that limits the search space of the algorithm within the maximum power point containing the area. Limitation of the algorithm's search space narrowed the response time to the changing weather conditions that in return declines the steady-state oscillations at the MPP.
(Killi and Samanta, 2015) [20]	Drift-free P&O algorithm	Duty ratio, dynamic perturbation	SEPIC converter	Suggested approach in this paper is the avoidance of drift for varying irradiance to track MPP accurately. As, the authors concluded that simple P&O algorithm undergoes a drift due to wrong decision-making capacity of the algorithm, in high solar insolation.
(Tang et al., 2017) [21]	Model predictive control	MPC duty cycle	Boost converter	MPC based MPPT algorithm is proposed for the large-scale marine PV system. The system makes the maximum solar energy utilization possible by overcoming the varying nature of partial shadings.
(Kchaou et al., 2017) [22]	Second order sliding mode control	Duty ratio	Boost converter	A robust MPPT algorithm is presented that uses second order sliding mode control strategy. The outcomes prove that the algorithm provides fast response and less chattering under varying atmosphere.
(Chaieb and Sakly, 2018) [23]	Simplified Accelerated Particle Swarm Optimization	Duty cycle	Buck converter	The study suggested a modified particle swarm optimization algorithm. The results show that the proposed approach is able to track the GMPP, especially under the partial shading conditions.
(Kamran et al. 2018) [5]	LabVIEW Based variable step sized P&O	Duty cycle	Boost converter	The authors developed a solar cell simulator integrated with variable step sized P&O algorithm on LabVIEW.
(Al-Dhaifallah et al., 2018) [24]	Fractional order control based incremental conductance	Duty cycle	Boost converter	The paper presents a fractional order control based incremental conductance MPPT algorithm. The results show high tracking accuracy for remarkable climate changes. The integration of the fractional order control with the conventional INC algorithm increases the tracking speed by 41.67%.
(El Khazane and Tissir, 2018) [25]	Finite Time Sliding Mode Control (FTSMC)	Duty cycle	DC-DC converter	The proposed FTSMC MPPT technique ensures the fast error tracking capability for the PV pumping system.
(Hifsa et al. 2018) [26]	Incremental Conductance integrated with a temperature	Duty cycle	Boost converter	The authors proposed a maximum power point tracker based on Incremental conductance algorithm integrated with an optical temperature

	controller			controller for an indoor PV system.
(Alik and Jusoh, 2018) [27]	Variable step size P&O	Duty cycle	Boost converter	A modified P&O algorithm is observed to increase the efficiency of the system by 16 % in partial shading conditions.

## 5. Conclusion

Varying solar irradiance and the temperature of the solar cell directly affects the performance of the solar system. This document presents a simple MPPT procedure to track the GMPP simulated in MATLAB/Simulink. The simulation results completely validate the solidity of the proposed technique by guaranteeing the meeting of operating points to GMPP under modified input/output circumstances of the PV structure. Simulation results confirm that the projected algorithm is faster and more precise than the existing algorithms. We have exposed that in normal weather circumstances, MPP is tracked in 0.1 seconds, and after that under partial conditions, the algorithm tracks GMPP in 0.15 seconds. Hence, the proposed MPPT algorithm not only reduced the tracking time but also minimized the oscillations at the maximum power point.

## References

- [1] F. Lasnier, Photovoltaic engineering handbook: Routledge, 2017.
- [2] M. H. Rehmani, M. Reisslein, A. Rachedi, M. Erol-Kantarci, and M. Radenkovic, "Integrating Renewable Energy Resources Into the Smart Grid: Recent Developments in Information and Communication Technologies," IEEE Transactions on Industrial Informatics, vol. 14, pp. 2814-2825, 2018.
- [3] N. Karami, N. Moubayed, and R. Outbib, "General review and classification of different MPPT Techniques," Renewable and Sustainable Energy Reviews, vol. 68, pp. 1-18, 2017/02/01/ 2017.
- [4] P. Soulatiantork, L. Cristaldi, M. Faifer, C. Laurano, R. Ottoboni, and S. Toscani, "A tool for performance evaluation of MPPT algorithms for photovoltaic systems," Measurement, vol. 128, pp. 537-544, 2018/11/01/ 2018.
- [5] M. Kamran, M. Bilal, and Z. J. Zaib, "LabVIEW Based Simulator for Solar Cell Characteristics and MPPT Under Varying Atmospheric Conditions," Mehran University Research Journal of Engineering and Technology; Vol 37 No 3 (2018): July Issue DO - 10.22581/muet1982.1803.07, 07/01 2018.
- [6] H. Nademi, Z. Soghomonian, and L. Norum, "A robust predictive MPPT strategy: An enabler for improving the photovoltaic conversion source," in 2017 IEEE 6th International Conference on Renewable Energy Research and Applications (ICRERA), 2017, pp. 1086-1091.
- [7] M. Kamran, M. R. Fazal, M. Mudassar, S. R. Ahmed, M. Adnan, I. Abid, et al., "Solar Photovoltaic Grid Parity: A Review of Issues, Challenges and Status of Different PV Markets," International Journal of Renewable Energy Research (IJRER), vol. 9, pp. 244-260, 2019.
- [8] L. Gao, R. A. Dougal, S. Liu, and A. P. Iotova, "Parallel-Connected Solar PV System to Address Partial and Rapidly Fluctuating Shadow Conditions," IEEE Transactions on Industrial Electronics, vol. 56, pp. 1548-1556, 2009.
- [9] A. H. El-Din, S. F. Mekhamer, and H. M. El-Helw, "Maximum power point tracking under partial shading condition using particle swarm optimization with DC-DC boost converter," in 2018 53rd International Universities Power Engineering Conference (UPEC), 2018, pp. 1-6.
- [10] K. Amara, A. Fekik, D. Hocine, M. L. Bakir, E. Bourennane, T. A. Malek, et al., "Improved Performance of a PV Solar Panel with Adaptive Neuro-Fuzzy Inference System ANFIS based MPPT," in 2018 7th International Conference on Renewable Energy Research and Applications (ICRERA), 2018, pp. 1098-1101.
- [11] R. Ramaprabha, M. Balaji, and B. L. Mathur, "Maximum power point tracking of partially shaded solar PV system using modified Fibonacci search method with the fuzzy controller," International Journal of Electrical Power & Energy Systems, vol. 43, pp. 754-765, 2012/12/01/ 2012.
- [12] S. Malathy and R. Ramaprabha, "Maximum power point tracking algorithm of SPVA under inhomogeneous irradiation conditions: A modified Fibonacci search-based approach," in 2017 IEEE 12th International Conference on Power Electronics and Drive Systems (PEDS), 2017, pp. 487-492.
- [13] M. Tsai, C. Chu, and W. Chen, "Implementation of a Serial AC/DC Converter With Modular Control Technology," in 2018 7th International Conference on Renewable Energy Research and Applications (ICRERA), 2018, pp. 245-250.
- [14] C. Wei-Ru, L. Chen, W. Chia-Hsuan, and L. Ci-Min, "Multiclustor-based particle swarm optimization algorithm for photovoltaic maximum power point tracking," in 2015 IEEE 2nd International Future Energy Electronics Conference (IFEEEC), 2015, pp. 1-6.
- [15] M. Mao, Q. Duan, L. Zhang, H. Chen, B. Hu, and P. Duan, "Maximum Power Point Tracking for Cascaded PV-Converter Modules Using Two-Stage Particle Swarm Optimization," Scientific Reports, vol. 7, p. 9381, 2017/08/24 2017.
- [16] K. Kajiwara, N. Matsui, and F. Kurokawa, "A new MPPT control for solar panel under bus voltage fluctuation," in 2017 IEEE 6th International Conference

- on Renewable Energy Research and Applications (ICRERA), 2017, pp. 1047-1050.
- [17] K. Kajiwara, H. Tomura, N. Matsui, and F. Kurokawa, "Performance-Improved Maximum Power Point Tracking Control for PV System," in 2018 7th International Conference on Renewable Energy Research and Applications (ICRERA), 2018, pp. 1153-1156.
- [18] M. Kamran, M. Mudassar, M. R. Fazal, M. U. Asghar, M. Bilal, and R. Asghar, "Implementation of improved Perturb & Observe MPPT technique with confined search space for standalone photovoltaic system," *Journal of King Saud University - Engineering Sciences*, 2018/06/18/ 2018.
- [19] A. Zbeeb, V. Devabhaktuni, and A. Sebak, "Improved photovoltaic MPPT algorithm adapted for unstable atmospheric conditions and partial shading," in 2009 International Conference on Clean Electrical Power, 2009, pp. 320-323.
- [20] M. Killi and S. Samanta, "Modified Perturb and Observe MPPT Algorithm for Drift Avoidance in Photovoltaic Systems," *IEEE Transactions on Industrial Electronics*, vol. 62, pp. 5549-5559, 2015.
- [21] R. Tang, Z. Wu, and Y. Fang, "Configuration of marine photovoltaic system and its MPPT using model predictive control," *Solar Energy*, vol. 158, pp. 995-1005, 2017/12/01/ 2017.
- [22] A. Kchaou, A. Naamane, Y. Koubaa, and N. M'sirdi, "Second-order sliding mode-based MPPT control for photovoltaic applications," *Solar Energy*, vol. 155, pp. 758-769, 2017/10/01/ 2017.
- [23] H. Chaieb and A. Sakly, "A novel MPPT method for photovoltaic application under partial shaded conditions," *Solar Energy*, vol. 159, pp. 291-299, 2018/01/01/ 2018.
- [24] M. Al-Dhaifallah, A. M. Nassef, H. Rezk, and K. S. Nisar, "Optimal parameter design of fractional order control based INC-MPPT for PV system," *Solar Energy*, vol. 159, pp. 650-664, 2018/01/01/ 2018.
- [25] J. El Khazane and E. H. Tissir, "Achievement of MPPT by finite time convergence sliding mode control for photovoltaic pumping system," *Solar Energy*, vol. 166, pp. 13-20, 2018/05/15/ 2018.
- [26] H. Shahid, M. Kamran, Z. Mehmood, M. Y. Saleem, M. Mudassar, and K. Haider, "Implementation of the novel temperature controller and incremental conductance MPPT algorithm for indoor photovoltaic system," *Solar Energy*, vol. 163, pp. 235-242, 2018/03/15/ 2018.
- [27] R. Alik and A. Jusoh, "An enhanced P&O checking algorithm MPPT for high tracking efficiency of partially shaded PV module," *Solar Energy*, vol. 163, pp. 570-580, 2018/03/15/ 2018.